Structural Eng. / Earthquake Eng. Vol. 3. No. 2, 247s-255s. October 1986
Japan Society of Civil Engineers (Proc. of JSCE No. 374/I-6)

NONLINEAR RESPONSE OF A RECTANGULAR PLATE SUBJECTED TO INPLANE DYNAMIC MOMENT

By Kazuo TAKAHASHI, Yasunori KONISHI**,*
*Torahiko IKEDA*** and Ryuta KAWANO*****

In the present paper, the vibration of the web plate under sinusoidally time-varying inplane moment is examined from the point of view of dynamic instability. The web plate is idealized by one rectangular plate surrounded by the upper and lower flange plates and vertical stiffeners. Inplane static and sinusoidally time-varying moments act on the edges of the plate. The dynamic instability regions are analyzed by the small deflection theory of thin plate. The amplitudes of unstable motions are determined by large deflection theory considering geometric nonlinearity.

Numerical results are presented for various boundary conditions, loading conditions and dampings of the plate.

Keywords : dynamic stability, nonlinear analysis, vibration of plate

1. INTRODUCTION

Fatigue failure of welded plate girder bridges at the welded joint connecting the web and flange plates and the generation of undesired acoustic radiation are found under dynamic loading[1),2)]. It is clear that these phenomena are due to out-of-plane vibrations of the web plate under time-varying inplane bending moment, caused by initial imperfection of the web plate or dynamic instability of the web plate.

As to the influence of initial imperfection, comprehensive studies have been performed by Maeda et al.[1)]. On the other hand, dynamic instability of the web plate is not treated theoretically, although Kuranishi et al.[2)] treated this problem by time response analysis. It is still not clear whether the dynamic instability exists or not.

In this study, the dynamic instability of the web plate under inplane sinusoidally time varying moment is examined. The web plate is idealized by a rectangular plate which is surrounded by upper and lower flange plates and vertical stiffeners. Inplane static and sinusoidally time-varying moments caused by static and dynamic girder bending act on the edges of the plate.

The dynamic instability which are determined by the small deflection theory has been presented in reference[3)]. The results led to the following conclusions : (1) combination resonances are predominant for the present case : this fact is different from those of the uniformly distributed loaded plate which has simple resonances only : the widths of the stable regions are broad when natural frequencies are close to

* Member of JSCE, Dr. Eng., Associate Professor, Department of Civil Engineering, Nagasaki University (Bunkyo-machi 1-14, Nagasaki City, Nagasaki)
** Member of JSCE, Dr. Eng., Professor, Department of Civil Engineering, Nagasaki University (Bunkyo-machi 1-14, Nagasaki City, Nagasaki)
*** Member of JSCE, M. Eng., Chodai Co. (Fukuoka City, Fukuoka)
**** Member of JSCE, Graduate Student of Nagasaki University (Bunkyo-machi 1-14, Nagasaki City, Nagasaki)

each other independently of the boundary conditions and aspect ratios; (2) the static moment has influenced upon the unstable region : the simple resonances whose widths are narrow in the absence of static moment become broad.

According the these results, the dynamic properties of the plate subjected to inplane dynamic moment are clearified for various parameters. The amplitudes of unstable regions become infinite under the assumptions of the small deflection theory. However, these amplitudes are bounded because of the stretching of the middle plane of the plate. From this fact, the amplitudes of unstable motions must be estimated by the large deflection theory of the plate.

The purpose of the present paper is to present an analytical approach to the investigation of nonlinear response of a rectangular plate subjected to the inplane dynamic moment. The equation of motion describing large deflection of the plate is analyzed by the Galerkin method. The resulting equations for time variables are integrated by using the Runge-Kutta-Gill method. Numerical results are presented for various boundary conditions, loading conditions and dampings.

2. GOVERNING EQUATIONS AND BOUNDATY CONDITIONS

Cartesian coordinate system (x, y) is introduced as shown in Fig. 1.

Static moment M_0 and sinusoidally time-varying moment $M_t \cos \Omega t$ act on two edges, $x=0$ and a. Inplane force N_x due to these moments is given by

$$N_x=\frac{6}{b^2}\left(1-2\frac{y}{b}\right)(M_0+M_t\cos\Omega t) \cdots\cdots (1)$$

where b is the length of the loaded edge, and Ω and M_t are the forcing circular frequency and the amplitude of the sinusoidally time-varying moment.

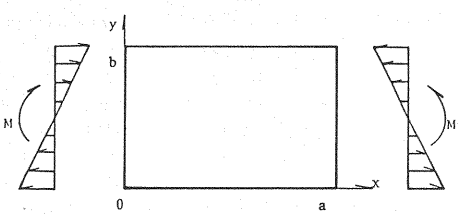

Fig. 1 Geometry and coordinate system.

Assuming that the effects of longitudinal and rotatory inertia forces and transverse shear can be neglected, then the basic equations for large amplitude free vibrations of a plate subjected to an inplane moment can be written as

$$L(w,F)=\rho d\frac{\partial^2 w}{\partial t^2}+D\nabla^4 w-\frac{6}{b^2}\left(1-2\frac{y}{b}\right)(M_0+M_t\cos\Omega t)\frac{\partial^2 w}{\partial x^2}$$
$$-d\left(\frac{\partial^2 F}{\partial y^2}\frac{\partial^2 w}{\partial x^2}+\frac{\partial^2 F}{\partial x^2}\frac{\partial^2 w}{\partial y^2}-2\frac{\partial^2 F}{\partial x\partial y}\frac{\partial^2 w}{\partial x\partial y}\right)=0 \cdots\cdots (2)$$

$$\nabla^4 F=E\left\{\left(\frac{\partial^2 w}{\partial x\partial y}\right)^2-\frac{\partial^2 w}{\partial x^2}\frac{\partial^2 w}{\partial y^2}\right\} \cdots\cdots (3)$$

where w denotes the plate deflection, ρ the mass density, d the plate thickness, t the time, $D=Ed^3/\{12(1-\nu^2)\}$ the bending stiffness, E Young's modulus, ν Poisson's ratio, and F Airy's stress function.

The following two boundary conditions for bending are considered in the present analysis :

Case I : simply supported along all edges; i. e.,

$$w=\frac{\partial^2 w}{\partial x^2}=0 \quad (x=0, a), \quad w=\frac{\partial^2 w}{\partial y^2}=0 \quad (y=0, b) \cdots\cdots (4\cdot a)$$

Case II : simply supported along the loaded edges and clamped along the other edges

$$w=\frac{\partial^2 w}{\partial x^2}=0 \quad (x=0, a), \quad w=\frac{\partial w}{\partial y}=0 \quad (y=0, b) \cdots\cdots (4\cdot b)$$

With regard to inplane boundary conditions, all edges are immovable. Since it is difficult to satisfy the inplane constraints exactly, the average inplane constraint boundary conditions are employed as

$$\int_0^b u dy=0 \quad (x=0, a), \quad \int_0^a v dx=0 \quad (y=0, b) \cdots\cdots (5)$$

where

$$u=\int_0^x \frac{\partial u}{\partial x}\,dx=\int_0^x \left\{\frac{1}{E}\left(\frac{\partial^2 F}{\partial y^2}-\nu\frac{\partial^2 F}{\partial x^2}\right)-\frac{1}{2}\left(\frac{\partial w}{\partial x}\right)^2\right\}dx$$

$$v=\int_0^y \frac{\partial v}{\partial y}\,dy=\int_0^y \left\{\frac{1}{E}\left(\frac{\partial^2 F}{\partial x^2}-\nu\frac{\partial^2 F}{\partial y^2}\right)-\frac{1}{2}\left(\frac{\partial w}{\partial y}\right)^2\right\}dy$$

3. METHOD OF SOLUTION

Taking these boundary conditions into account, we assume the solution of equation (2) by

$$w=d\sum_{n=1} T_{Mn}(t)\,W_{Mn}(x,y) \quad \cdots\cdots (6)$$

where T_{Mn} is an unknown function of the time variable, and W_{Mn} an eigen-function associated with free vibrations satisfying the geometric boundary conditions of the plate, defined as

Case I : $$W_{Mn}=\sin\frac{M\pi x}{a}\sin\frac{n\pi y}{b} \quad \cdots\cdots (7\cdot a)$$

Case II : $$W_{Mn}=\sin\frac{M\pi x}{a}\sum_{i=1} a_i^n\left\{\cos\frac{(i-1)\pi y}{b}-\cos\frac{(i+1)\pi y}{b}\right\} \quad \cdots\cdots (7\cdot b)$$

The general solution of stress function F of equation (2) is expressed in the form

$$F=F_p+F_c \quad \cdots\cdots (8)$$

where F_p is the particular solution and F_c the complementary solution. Substituting equations (7·a) and (7·b) into equation (3), the particular solution F_p can be obtained (Appendix A).

Let the complemetary solution F_c be expressed in the form 4), 5) as

$$F_c=A(t)\,x^2+B(t)\,y^2 \quad \cdots\cdots (9)$$

where $A(t)$ and $B(t)$ are functions of time, which should be determined so that the inplane boundary condition (5) is satisfied (Appendix B).

After substituting equations (6) and (8) into equation (2), we apply a Galerkin method to obtain

$$\frac{\rho d b^4}{D}I^1_{Mp}\ddot{T}_{Mp}+I^2_{Mp}T_{Mp}+\frac{6}{D}(M_0+M_t\cos\Omega t)\sum_{n=1} I_{Mnp}T_{Mn}+\sum_{n=1}\sum_{r=1}\sum_{s=1} I_{Mnrsp}T_{Mn}T_{Mr}T_{Ms}=0 \quad \cdots\cdots (10)$$

where I^1_{Mp}, I^2_{Mp}, I_{Mnp} and I_{Mnrsp} are integrations that appear in the process of the Galerkin method (Appendix C) and $p=1, 2, \cdots$. Adding damping term and using nondimensional notations, we obtain the following differential equation for the time variable :

$$\ddot{T}_{Mp}+2h^M_p\left(\frac{\omega^M_p}{\omega^1_1}\right)\dot{T}_{Mp}+\left(\frac{\omega^M_p}{\omega^1_1}\right)^2 T_{Mp}+(\overline{M}_0+\overline{M}_t\cos\overline{\omega}\tau)\sum_{n=1} A_{Mnp}T_{Mn}+\sum_{n=1}\sum_{r=1}\sum_{s=1} B_{Mnrsp}T_{Mn}T_{Mr}T_{Ms}=0 \quad \cdots\cdots (11)$$

where $\overline{M}_0=M_0/M_{cr}$ is the nondimensional static moment, $\overline{M}_t=M_t/M_{cr}$ the nondimensional dynamic moment, $M_{cr}=\lambda_{cr}\pi^2 D/6$ the buckling moment, λ_{cr} the eigenvalue of the buckling moment, $\overline{\omega}=\Omega/\Omega^1_1$ the nondimensional forcing circular frequency, $\Omega^1_1=\pi^2/b^2\sqrt{D/\rho d}$ the first natural circular frequency, α^1_1 the first eigenvalue of vibration, $\tau=\Omega^1_1 t$ the nondimensional time, h^M_p the damping constant, and ω^M_p the p-th natural circular frequency with the half wave number M. A_{Mnp} and B_{Mnrsp} are given in Appendix D.

4. METHOD OF TIME RESPONSE ANALYSIS

The coefficient A_{Mnp} of parametric exciatations of the present case is shown (see chapter 4. of reference 3), p. 181) :

$A_{Mnn}=0.0$, $A_{Mnp}=0.0$ $(n+p=$even number$)$ and $A_{Mnp}\neq 0.0$ $(n+p=$odd number$)$ $\cdots\cdots$ (12)

In the present problem, the diagonal element A_{Mnn} is zero. Parametric resonances occur only through the coupling term $A_{Mnp}(n\neq p)$. Therefore, simple parametric resonance[3] which occurs through the direct term A_{Mnn} would not be important for the present case. Combination resonances[3] which occur through the non-zero coupling terms are predominant. As the coefficient is symmetric, $A_{Mnp}=A_{Mpn}$, combination resonances with sum type can be appeared only. As the non-zero elements are A_{M12}, A_{M14}, A_{M23} and so on, combination resonances such as $\omega^M_1+\omega^M_2$, $\omega^M_1+\omega^M_4$, $\omega^M_2+\omega^M_3$, etc. are contained.

The combination resonance is vibration of the two degrees-of-freedom system. The two degrees-of-freedom approach is adopted to obtain a time response. Time variables are integrated numerically by using the Runge-Kutta-Gill method. The purpose of the present analysis is to determine the amplitudes of unstable motions which occur under the assumptions of the small deflection theory. Therefore, the initial conditions for time variables are $T_{Mi}=T_{Mj}=0.01$ and $\dot{T}_{Mi}=\dot{T}_{Mj}=0.00$ to satisfy the small amplitude vibration. Poisson's ratio ν of the plate is taken as 0.3.

5. NUMERICAL RESULTS

(1) Effect of boundary conditions

Fig. 2 and 3 show unstable regions of a square plate ($\mu=1.0$) for case I and case II which are obtained by the linear analysis[3] (These figures are the same as Fig. 4 and 5, pp. 182~183). In these figures, the abscissa $\overline{\omega}$ shows the nondimensional forcing frequency and the ordinate $\overline{M}_t$ indicates the nondimensional moment. Combination resonances of sum type in the vicinity of $\omega_i^M+\omega_j^M$ are obtained. The diagonal elements of the coefficient A_{Mnn} are zero in the present problem. However, the secondary unstable regions of the simple resonances such as ω_i^M occur through coupling terms. The widths of simple resonances are narrower than those of combination resonances. Therefore, combination resonances are important for the present problem. The widths of combination resonances with closed natural frequencies are broad such as $\omega_1^2+\omega_2^2$ for case I and $\omega_1^3+\omega_2^3$ for case II.

The amplitudes of these unstable regions obtained by linear analysis tend toward infinity (see Fig. 6 of reference 3) p. 183). Nonlinear time responses for the combination resonances $\omega_1^1+\omega_2^1$ and simple resonance ω_2^2 are shown in Fig. 4 and 5. Amplitudes are bounded due to the nonlinear terms effect which is caused by inplane forces due to the deflection of the plate. Beating can be seen in the nonlinear parametric dynamic system. This beating is obtained in the single degree-of-freedom system as well as in the two degrees-of-freedom system, as can be found later in Fig. 15 in this paper. It is concluded that this phenomenon is attributed to the basic properties of the nonlinear parametric dynamic system.

The maximum amplitudes of beating for each central frequency $\omega_i^M+\omega_j^M$ or ω_i^M of the unstable motions are shown in Fig. 6 and 7. In these figures, the abscissa $\overline{M}_t$ shows the nondimensional moment and the ordinate

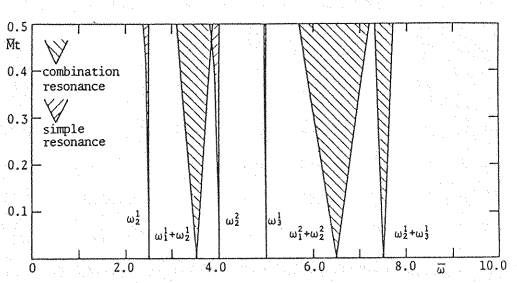

Fig. 2 Unstable regions of a square plate : case I and $\overline{M}_0=0.0$.

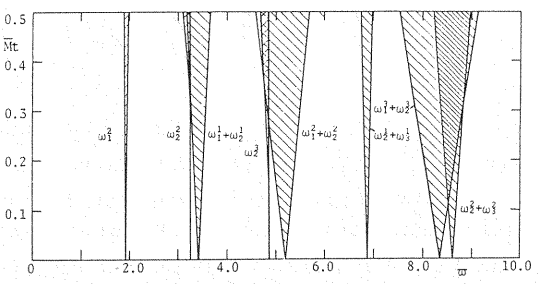

Fig. 3 Unstable regions of a square plate : case II and $\overline{M}_0=0.0$.

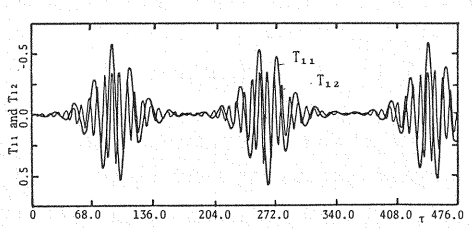

Fig. 4 Time history of the combination resonance : case I, $\omega_1^1+\omega_2^1$, $\overline{M}_t=0.5$ and $\overline{\omega}=3.5$.

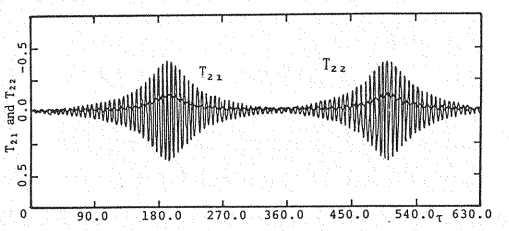

Fig. 5 Time history of the simple resonance : case I, ω_2^2, $\overline{M}_t=0.5$ and $\overline{\omega}=4.0$.

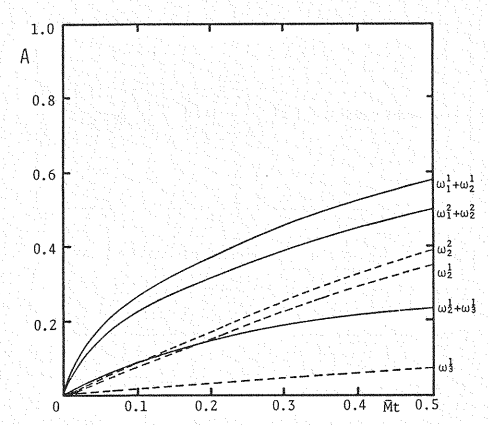

Fig. 6 Maximum amplitudes of unstable motions : case I and $\overline{M}_0=0.0$.

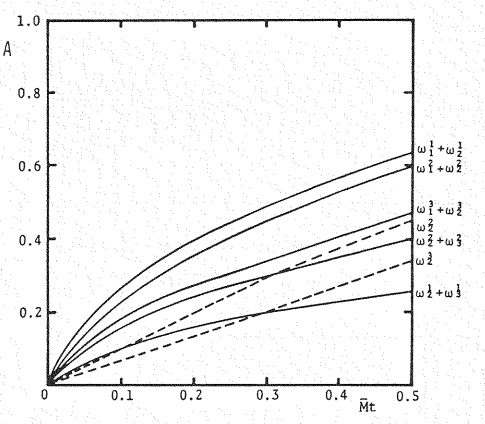

Fig. 7 Maximum amplitudes of unstable motions : case II and $\overline{M}_0=0.0$.

A indicates the maximum amplitude which is nondimensionalized by the plate thickness d. The amplitudes of the combination resonances are greater than those of the simple resonances and become smaller in the order of $\omega_1^1+\omega_2^1$, $\omega_1^2+\omega_2^2$, $\omega_2^1+\omega_3^1$ for case I and $\omega_1^1+\omega_2^1$, $\omega_1^2+\omega_2^2$, $\omega_1^3+\omega_2^3$, $\omega_2^2+\omega_3^2$, $\omega_2^1+\omega_3^1$ for case II. The amplitudes of combination resonance, that is, $\omega_1^1+\omega_2^1$ for case I and II which occurs at the lowest frequency range as can be seen in Fig. 2 and 3 are the maxiam. The maximum amplitudes occur when the sum of ω_i^M and ω_j^M is a minimum and are not directly dependent on the width of the unstable regions as show in Fig. 2 and 3. The maximum amplitudes are not much affected by the differences in the boundary conditions, case I and case II.

(2) Effect of static moment

Fig. 8 shows unstable regions of a square plate subjected to static moment $\overline{M}_0=0.3$ (see Fig. 9 of reference 3) p. 184). Simple resonances with $2\omega_1^1$, $2\omega_1^2$ and $2\omega_1^3$ occur through the fourth term $\overline{M}_0\sum_{n=1} A_{MnP}T_{Mn}$ of equation (11). This result corresponds to the fact that the coupling between modes occurs through the linear restoring force term. The amplitudes of the present case are shown in Fig. 9. The static moment $\overline{M}_0$ has influence upon the amplitudes of unstable motions. As the effect of the static moment $\overline{M}_0$ decreases the stiffness of the plate, the amplitudes of Fig. 9 which includes the static moment $\overline{M}_0$ become greater in general than those of Fig. 6. However, there is one exception, i.e., combination resonance $\omega_1^2+\omega_2^2$. The amplitudes of the combination resonances $\omega_1^2+\omega_2^2$ increase rapidly when the moment

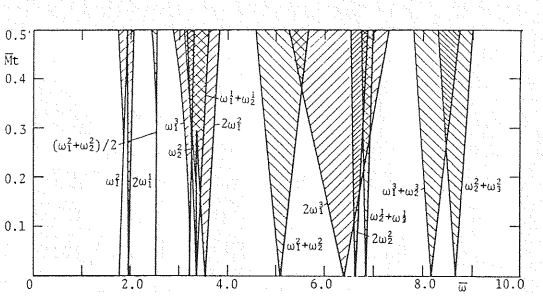

Fig. 8 Unstable regions of a square plate : case II and $\overline{M}_0=0.3$.

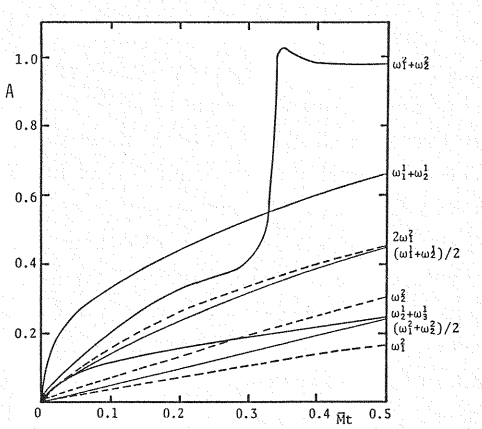

Fig. 9 Maximum amplitudes of unstable motions : case I and $\overline{M}_0=0.3$.

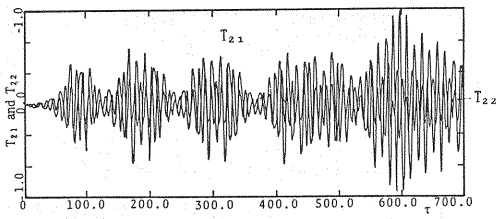

Fig. 10 Time history of the combination resonance : case Ⅱ, $\omega_2^2+\omega_2^2$, $\overline{M}_0=0.3$, $\overline{M}_t=0.5$ and $\overline{\omega}=6.4$.

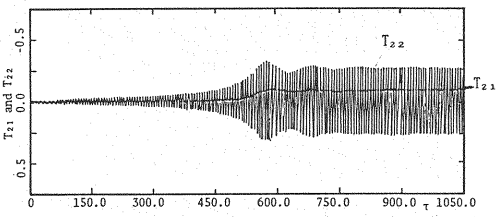

Fig. 13 Time history of the simple resonance : case Ⅰ, ω_2^2, $h=0.01$, $\overline{M}_t=0.5$ and $\overline{\omega}=4.0$.

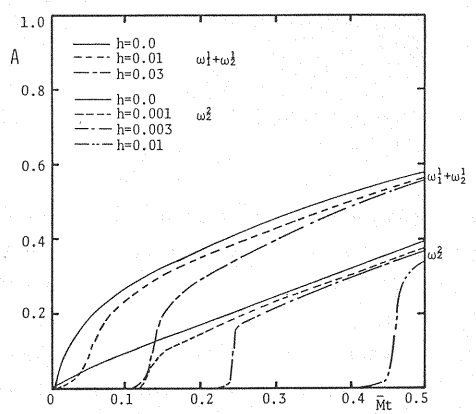

Fig. 11 Effect of damping on the maximum amplitudes : case Ⅰ and $\overline{M}_0=0.0$.

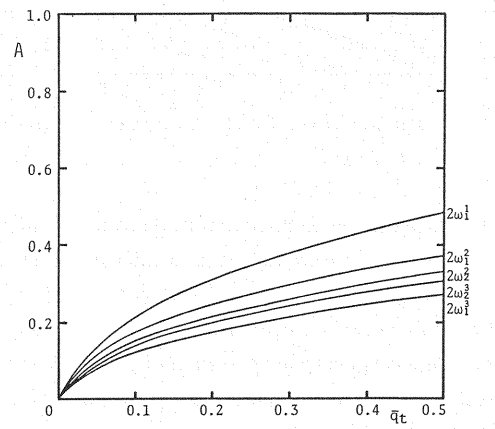

Fig. 14 Maximum amplitudes of unstable motions : case Ⅱ and $\overline{q}_0=0.0$.

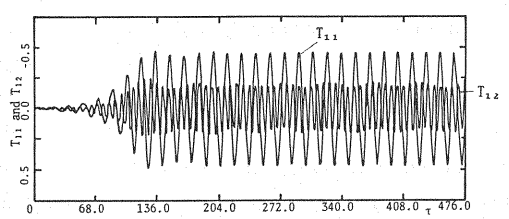

Fig. 12 Time history of the combination resonance : case Ⅰ, $\omega_1^1+\omega_2^1$, $h=0.03$, $\overline{M}_t=0.5$ and $\overline{\omega}=3.5$.

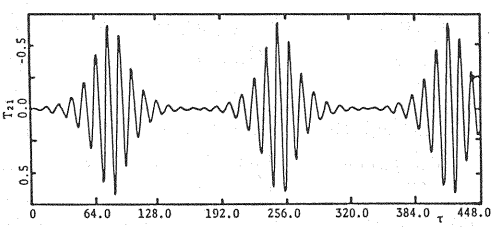

Fig. 15 Time history of the simple resonance : case Ⅰ, $2\omega_1^2$, $\overline{q}_t=0.5$ and $\overline{\omega}=3.782$.

$\overline{M}_t$ is greater than 0.3 as shown in Fig. 9. The nonlinear time response of this type of vibration is shown in Fig. 10. The maximum response occurs after several beatings. This pattern can be observed only in the case of the combination resonance $\omega_1^2+\omega_2^2$. The half wave number $M=2$ of this unstable vibration coincides with that of the buckling problem due to static moment $M_0=M_{cr}$. It is assumed that the dynamic buckling occurs under the actions of static and dynamic moments.

(3) Effect of damping

In the linear case, the effect of damping varies depending on the width of the unstable region. Narrow unstable regions become stable due to the damping effect (see Fig. 12 of reference 3), p. 185). Amplitudes of the combination resonance $\omega_1^2+\omega_2^2$ and the simple resonance ω_2^2 for various magnitudes of damping constant ($h_i^M=h_j^M=h$) are shown in Fig. 11. The damping of the simple resonance are assumed to be one tenth of those of the combination resonance since the simple resonance is much affected by magnitude of damping. The effect of damping decreases the amplitudes of unstable motions and this tendency is conspicuous where the exciting moment $\overline{M}_t$ is small. The unstable motion does not occur if the damping effect is greater than the divergence (negative damping) effect of the parametric instability. The effect of

damping becomes smaller with increase of the moment $\overline{M}_t$. The nonlinear time responses of the damped parametric system are shown in Fig. 12 and 13. The amplitudes of the damped system reach their maximum value without beating.

(4) Effect of loading condition

Fig. 14 shows the nonlinear response of a square plate subjected to uniformly distributed load. As the simple parametric resonances are contained only in the present case[6], amplitudes of the simple parametric resonances are obtained. Fig. 15 shows nonlinear time response of $2\omega_1^2$. As the simple parametric resonance is unstable motion of the single degree-of-freedom, the only one time variable is excited.

6. CONCLUSIONS

The present paper shows the nonlinear dynamic instability of a rectangular plate subjected to inplane dynamic moment.

The conclusions are as follows :

(1) Amplitudes of the out-of-plane vibrations of a rectangular plate subjected to an inplane dynamic moment are bounded due to geometric nonlinear term effect. Nonlinear time responses of unstable motions accompany beating.

(2) Amplitudes of combination resonances are greater than those of simple parametric resonances for the present case. This fact is quite different from those of the uniformly distributed loaded plate which has simple resonances only.

(3) Effect of static moment increases amplitudes of unstable motions in general. Amplitudes of the combination resonance whose modal shape is similar to that of the buckled mode is much affected by static moment.

(4) Effect of damping decreases the amplitude of unstable motions. This effect is conspicuous where the parametric excition moment is small.

Appendix A : Particular Solution F_p of Equation (8).

$$F_p=Ed^2\sum_{n=1}\sum_{s=1}T_{Mn}T_{Ms}F^p_{Mns}$$

where

Case Ⅰ :

$$F^p_{Mns}=A^M_{ns}\cos(n-s)\pi\eta+B^M_{ns}\cos(n+s)\pi\eta+\cos 2M\pi\xi\{C^M_{ns}\cos(n-s)\pi\eta+D^M_{ns}\cos(n+s)\pi\eta\}$$

$$A^M_{ns}=\frac{M^2 s}{4\mu^2(n-s)^3},\quad B^M_{ns}=\frac{M^2 s}{4\mu^2(n+s)^3},\quad C^M_{ns}=\frac{\mu^2M^2(n+s)s}{4\{4M^2+(n-s)^2\mu^2\}^2},$$

$$D^M_{ns}=\frac{\mu^2M^2(n-s)s}{4\{4M^2+(n+s)^2\mu^2\}^2},\quad \text{in which}\quad A^M_{ns}=0\quad (n=s),$$

$$\xi=x/a,\quad \eta=y/b,\quad \mu=a/b\quad \text{(aspect ratio)}$$

Case Ⅱ :

$$\begin{aligned}F^p_{Mns}=\sum_{i=1}\sum_{j=1}a^n_i a^s_j[&A^M_{ij}\cos(i-j)\pi\eta+B^M_{ij}\cos(i+j)\pi\eta+C^M_{ij}(i+j-2)\pi\eta\\&+D^M_{ij}\cos(i-j+2)\pi\eta+E^M_{ij}\cos(i-j-2)\pi\eta+F^M_{ij}\cos(i+j+2)\pi\eta\\&+\cos 2\pi\xi\{G^M_{ij}\cos(i-j)\pi\eta+H^M_{ij}\cos(i+j)\pi\eta+I^M_{ij}\cos(i+j-2)\pi\eta\\&+J^M_{ij}\cos(i-j+2)\pi\eta+K^M_{ij}\cos(i-j-2)\pi\eta+L^M_{ij}\cos(i+j-2)\pi\eta\}]\end{aligned}$$

$$A^M_{ij}=\frac{M^2 j}{2\mu^2(i-j)^3},\quad B^M_{ij}=\frac{M^2 j}{2\mu^2(i+j)^3},\quad C^M_{ij}=\frac{M^2(1-j)}{4\mu^2(i+j-2)^3},$$

$$D^M_{ij}=\frac{M^2(1-j)}{4\mu^2(i-j+2)^3},\quad E^M_{ij}=\frac{-M^2(1-j)}{4\mu^2(i-j-2)^3},\quad F^M_{ij}=\frac{-M^2(1-j)}{4\mu^2(i+j+2)^3},$$

$$G^M_{ij}=\frac{\mu^2M^2(ij+j^2+2)}{2\{4M^2+(i-j)^2\mu^2\}^2},\quad H^M_{ij}=\frac{\mu^2M^2(ij-j^2-2)}{2\{4M^2+(i+j)^2\mu^2\}^2},\quad I^M_{ij}=\frac{\mu^2M^2(i-j)(1-j)}{4\{4M^2+(i+j-2)^2\mu^2\}^2},$$

$$J^M_{ij}=\frac{\mu^2M^2(i+j)(1-j)}{4\{4M^2+(i-j+2)^2\mu^2\}^2},\quad K^M_{ij}=\frac{-\mu^2M^2(i+j)(1+j)}{4\{4M^2+(i-j-2)^2\mu^2\}^2},\quad L^M_{ij}=\frac{-\mu^2M^2(i+j)(1+j)}{4\{4M^2+(i+j+2)^2\mu^2\}^2}$$

in which $A^M_{ij}=0\ (i=j)$, $C^M_{ij}=0\ (i=j=1)$, $D^M_{ij}=0\ (i=j-2)$, $E^M_{ij}=0\ (i=j+2)$

Appendix B : Complementary Solution F_c of Equation (9).

$$F_c=Ed^2\sum_{n=1}\sum_{s=1}T_{Mn}T_{Ms}F^c_{Mns}$$

where

Case Ⅰ :

$$F^c_{Mns}=\frac{\pi^2\delta_{ns}}{16(1-\nu^2)}\{(\mu^2ns+\nu M^2)\xi^2+(M^2/\mu^2+\nu ns)\eta^2\}$$

Case Ⅱ :

$$F^c_{Mns}=\frac{\pi^2}{16(1-\nu^2)}[[a^n_1a^s_1(4\mu^2+3\nu M^2)+2\sum_{i=2}a^n_ia^s_i\{\mu^2(i^2+1)+\nu M^2\}-\sum_{i=1}a^n_ia^s_{i+2}\{\mu^2(i+1)^2+\nu M^2\}$$
$$-\sum_{i=3}a^n_ia^s_{i-2}\{\mu^2(i-1)^2+\nu M^2\}]\xi^2+[a^n_1a^s_1(4\nu+3M^2/\mu^2)+2\sum_{i=2}a^n_ia^s_i\{\nu(i^2+1)+M^2/\mu^2\}$$
$$-\sum_{i=1}a^n_ia^s_{i+2}\{\nu+(i+1)^2+M^2/\mu^2\}-\sum_{i=3}a^n_ia^s_{i-2}\{\nu(i-1)^2+M^2/\mu^2\}]\eta^2]$$

Appendix C : Integrations of the Galerkin Method

$$I^1_{Mp}=\int_0^1\int_0^1W^2_{Mp}\,d\xi d\eta$$

$$I^2_{Mp}=\int_0^1\int_0^1\left(\frac{1}{\mu^4}\frac{\partial^4W_{Mp}}{\partial\xi^4}+\frac{2}{\mu^2}\frac{\partial^4W_{Mp}}{\partial\xi^2\partial\eta^2}+\frac{\partial^4W_{Mp}}{\partial\eta^4}\right)W_{Mp}d\xi d\eta$$

$$I_{Mnp}=-\frac{1}{\mu^2}\int_0^1\int_0^1(1-2\eta)\frac{\partial^2W_{Mn}}{\partial\xi^2}W_{Mp}d\xi d\eta$$

$$I_{Mnrsp}=-\frac{12(1-\nu^2)}{\mu^2}\int_0^1\int_0^1\left(\frac{\partial^2F_{Mrs}}{\partial\eta^2}\frac{\partial^2W_{Mn}}{\partial\xi^2}-2\frac{\partial^2F_{Mrs}}{\partial\xi\partial\eta}\frac{\partial^2W_{Mn}}{\partial\xi\partial\eta}+\frac{\partial^2F_{Mrs}}{\partial\xi^2}\frac{\partial^2W_{Mn}}{\partial\eta^2}\right)W_{Mp}d\xi d\eta$$

$$F_{Mns}=F^p_{Mns}+F^c_{Mns}$$

Appendix D : Coefficients of Equation (11)

$$A_{Mnp}=I_{Mnp}/\{I^1_{Mp}(\alpha^1_1)^2\pi^2\}$$

$$B_{Mnp}=I_{Mnrsp}/\{I^1_{Mp}(\alpha^1_1)^2\pi^4\}$$

$$\omega^M_p=\sqrt{\frac{I^2_{Mp}}{I^1_{Mp}}\frac{D}{\rho db^4}}$$

RERERENCES

1) Maeda, Y. and Okura, I. : Effects of Initial Deflection of Fatigue Cracks due to Out-of-Plane Deflection of Thin Plate, Pro. of JSCE, No. 329, pp. 1~11, 1982.
2) Kuranishi, S., Fukaya, S. and Shima, T. : Vibration of Initially Deflected Web Plate under Periodic Beam Bending, Pro. of JSCE, No. 341, pp. 229~232, 1984.
3) Takahashi, K., Tagawa, M., Ikeda, T. and Matsukawa, T. : Dynamic Stability of a Rectangual Plate Subjected to Inplane Moment, Pro. of JSCE, No. 341, pp. 179~186, 1984.
4) Timoshenko, S. P. and Woinowsky-Krieger, S. : Theory of Plates and Shells, 2 nd Edition, McGraw-Hill Book Co., Inc., 1955.
5) Kanazawa, K. and Hangai, Y. : Nonlinear Flexural Vibrations of Thin Shallow Shells, Theoretical and Applied Mechanics, Vol. 25, pp. 75~87, 1975.

6) Yamaki, N. and Nagai, K. : Dynamic Stability of Rectangular Plates Using Periodic Compressive Forces, Rep. Inst. High Speed Mech., Tohoku Univ., Vol. 32, pp. 103～127, 1975.

(Received October 21 1985)